THE DECOMPOSITION KINETICS OF SOLIDS
PART 1: THE VARIATION OF THE KINETIC PARAMETERS

Akwilapo, L. D. and Kyobe, J. M. P.
Department of Chemistry, University of Dar es Salaam
P. O. Box 35061, Dar es Salaam

*U*nlike gas phase chemical reactions, solid state decompositions are characterised by; large values of activation energies, differences in reactivities of samples of the same reactant, variations of the kinetic parameters for the same chemical reaction and the localisation of the chemical reaction at the reaction interface. These factors, put together, indicate that, the traditional rate equation does not suffice in describing the behaviour of solid state decompositions, particularly in the determination of the kinetic parameters. In order to accommodate the problems surrounding solid state decomposition kinetics a new rate equation is proposed. The equation is used to determine the kinetic parameters in the decomposition of $CaCO_3$. The results show that the decomposition is a first order reaction, which is distorted by the cooling of the reaction environment in favour of heat transport, as the limiting process. The values of $A = 7 \times 10^8\ s^{-1}$ and $Ea = 217.5\ kJ\ mol^{-1}$ for the frequency factor and activation energy, respectively, have been obtained for the decomposition of $CaCO_3$.

Keywords: Solid state decomposition, Activation energy, Frequency factor.

INTRODUCTION

The obstacle to our understanding of the chemical reactivity of solids has not been due to the performance of the modern research tools, but because of lack of adequate consideration of the influence of the condensed state on the decomposition kinetics. A majority of solid state decomposition reactions are endothermic that are accompanied by the cooling of the reaction environment. This cooling of the reaction environment has a significant influence on the decomposition kinetics of solids, which is manifested in the decrease of the reaction rates, with increasing sample masses.

The traditional rate equation

$$\frac{d\alpha}{dt} = Af(\alpha)\exp\left(\frac{-E_a}{RT}\right) \qquad (1)$$

where $f(\alpha)$ is a function of the remaining fraction $(1 - \alpha)$ of the reactant, A the frequency factor, E_a the activation energy, R the universal gas constant and T the absolute temperature has always been applied in the analysis of solid state decompositions. The equation assumes that there is an equal energy distribution throughout the sample, the case that is true only in homogeneous kinetic studies, but not in solid state reactions. Such a scenario will also suggest that the rate constant, given by the equation,

$$k = A\exp\left(-E_a/RT\right) \qquad (2)$$

is fixed by temperature, which, as it will be shown here, it is not the case.

The variation of the results of kinetic studies, for solid state decompositions has been a subject of discussion for half a century now. The recent report by the ICTAC Kinetics Project [Maciejewski, 2000], and some other previous workers as reviewed by Garn [1978] and Dollimore et al., [1984] are all reporting on these discrepancies. According to Garn, the variation of the kinetic parameters A and E_a for solid state decompositions suggest that the Arrhenius

equation (2) cannot hold when the rate is a function of only temperature and the remaining fraction $(1 - \alpha)$. The argument implies that there has been no satisfactory kinetic model, which offers promising explanations regarding the behaviours of solid state decompositions. For this reason, we are arguing that, equation (1) is based on an incorrectly defined kinetic system in the elucidation of solid state decomposition reactions.

The results of kinetic studies of solid state decompositions unlike those of gas phase chemical reaction have shown that solid state decompositions have the following properties:

i.   they are always endothermic,

ii.   they have large values of the activation energies,

iii. the chemical reaction is localised at preferential sites (reaction interfaces),

iv.   the reactivities differ with sample masses for the same solid reactant, and

v.   there is a splitting of the chemical reaction giving a low initial chemical reaction followed by an acceleratory kinetic regime.

If homogeneous and solid state chemical reactions involve similar energy consuming processes, then it is puzzling to find out that for the same solid state chemical reaction different workers get varying kinetic parameters. This suggests that the extension of the energy barrier applicable in homogeneous kinetics is taken for granted in solid state decompositions. The conclusion may be that the rate equation (1) as suggested by Garn [1978] cannot hold in elucidating solid state decomposition reactions at all conditions. This statement is highly debatable because it will suggest that the kinetic parameters obtained should, therefore, be regarded as operational parameters devoid of any physical meaning. What a change from conventional thinking! The present contribution will discuss this paradox at length.

A kinetic model, which offers promising explanations, is proposed in this study. The model is tested in the decomposition kinetics of $CaCO_3$, a compound that has been extensively studied by various workers, but at each time different values of the kinetic parameters A and E_a, have being reported (Britton et al, 1952; Doyle, 1962; Berlin and Robinson, 1962; Ingraham and Marier, 1963; Speros and Woodhouse, 1968; Drapper and Sveum, 1970; Rouquerol and Rouquerol, 1972; Beruto and Searcy, 1974; Guler et. al., 1982; Dowdy, 1987). The different values of the activation energy, E_a, so reported by different workers, is hereby referred to as the apparent activation energy, E_a'. This apparent value is always lower than the actual one, i.e. $E_a' < E_a$. According to the model at hand, the population of reacting particles for a solid reactant, which can decompose at or above the threshold decomposition temperature T_o are localised at the reaction interface.

After acquiring an energy E_a', the reactant population at the reaction interface reach the activated state upon the extraction of the heat RT_o from the reaction environment. The absorption of heat by the reacting particles is inevitable due to the endothermic nature of the reaction. Of the total energy $E_a = E_a' + RT_o$, only RT_o gives the effective energy barrier. This is because the extraction of heat, RT_o, cools the immediate environment around the reaction surface and thereby rendering heat transport as the preferred rate limiting process. The routine rate equation (1) is therefore blind to this fundamental behaviour of solid state decomposition reactions.

Because the population of a solid reactant at the entire reaction interface is proportional to its area, the rate equation (1) for solid state decompositions should be proportional to the area of the reaction interface. This means that the rate would also vary depending on the area of the reaction interface, and not solely on the fraction decomposed, $f(\alpha)$, and temperature, T. For this reason sample masses of different sizes cannot react in the same way. Plots of α vs T shown in Figure 1 support this fact. The figure shows the reactivity of a solid reactant to vary with the sample mass. Since the rate is proportional to the area of the reaction interface of a solid reactant, equation (1) is therefore modified to equation (3):
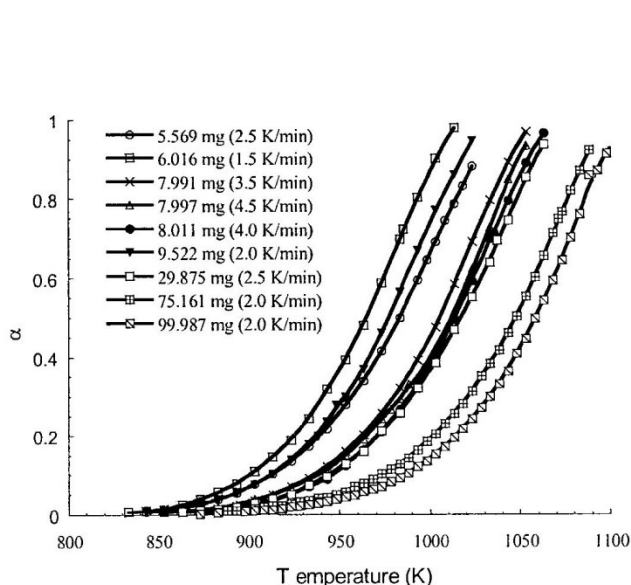
Figure 1: Typical plots of α vs T showing how the reactivity of a solid varies with sample mass and heating rate.

$$\frac{d\alpha}{dt} = \frac{af(\alpha)A'\exp\left(-E_a'/RT\right)}{a_0} \qquad (3)$$

where a_0 is the area of the reaction interface at the temperature T_0 of the start of the decomposition, a the area of the reaction interface at any other temperature T (greater than T_0) and A' and $E_{a'}$ are the apparent kinetic parameters.

In equation (3), the apparent kinetic parameters A' and E_a' are found to vary with the area of the reaction interface according to linear equations (4) and (5) respectively,

$$\ln A' = \ln A + a_0 X \dots \dots . \qquad .(4)$$

$$E_a' = E_a - a_0 RT \dots . . \qquad \dots (5)$$

In eqn. (4), x is the heat supply index, defined as the number of decompositions of the solid reactant per unit surface area of the reaction interface (cm^{-2}), which is determined graphically. Equation (3) was applied to the decomposition kinetics of $CaCO_3$ assuming the mechanism of a first order reaction. The area a of the reaction interface was calculated from the unreacted mass $m = m_0(1 - \alpha)$ and density d of the solid reactant. For a spherical geometry, we have,

$$a = Bm^{2/3} \qquad (6)$$

where B $= (36\pi/d^2)^{1/3}$ and d $= 2.71$ gcm^{-3} (Lide, 1992). Considering homogeneous kinetics, a comparison of the values of the frequency factor was made for two chemical reactions sharing a common mechanism. The comparison showed that the frequency factor of the order of 10^{13} s^{-1} is always obtained for first order gas phase chemical reactions (Trotman-Dickenson, 1959; Szwarc, 1961; Waters, 1961; Daniels, 1980). This finding is significant because it is possible to extend the comparison of the frequency factor to solid state decompositions in the elucidation of the mechanism of solid state decompositions. When a solid state decomposition is a first order reaction, the frequency factor should be of the order:

$$A_s = \frac{N_s A_g}{N_g} \qquad (7)$$

where $A_g = 10^{13}$ s^{-1} [Trotman-Dickenson, 1959; Szwarc, 1961; Waters, 1961; Daniels, 1980] and N_g is the population of the reacting particles (molecules) in 1 cm^3 of gas phase chemical reaction, equal to 2.68684 x 10^{19} molecules/cm^3. For $CaCO_3$, the number of planar CO_3^{2-} ions which can be assembled on 1 cm^2 of the reaction interface is $N_s = 1/\pi r^2 = 1.91285$ x 10^{15} calculated based on C-O distance r $= 1.29$ Å (Wells, 1962). Using these data, the frequency factor $A_s = 7.1$ x 10^8 s^{-1} is predicted for the decomposition of $CaCO_3$ according to a mechanism of a first order reaction

EXPERIMENTAL

The $CaCO_3$ used in this investigation was of analytical grade purity procured from May and Baker, Dagenham, England. The samples were cut and machined to desired sample sizes ranging from 6 to 100 mg. The thermogravimetric analyses of the samples were carried out on a Mettler TG50 thermobalance. The heating rates used ranged between 1.5 and

4.5 oC/min. A steady flow rate of 100 ml/min of nitrogen was maintained during the TG runs. In addition, before the experiments, the temperature calibration was carried out using recommended curie points of Isatherm (145 °C), Nickel (357 °C) and Trafoperm (748 °C).

RESULTS AND DISCUSSION

From the mass loss in TG curves, the decomposition of $CaCO_3$ can be expressed stoichiometrically as in equation (8) below,

$$CaCO_3(s) \rightarrow CaO(s) + CO_2(g) \qquad (8)$$
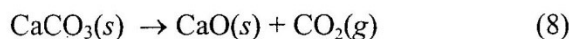
The kinetic measurements from the TG runs are presented in Table 1.

The Arrhenius plots constructed on the basis of the rate constants according to equation (3) are presented in Figure 2. The plots are linear for a range of α values followed by the kinetic break of the chemical reaction. For 5.969 and 99.997 mg samples, the plots are linear up to $\alpha = 0.60$ and 0.33, respectively. This indicates that the rate equation (3) is obeyed up to certain extent of decomposition. The result shows the decrease of the apparent kinetic parameters with the increase of the sample mass, which suggests that the decomposition reaction is accompanied by the cooling of the reaction environment.

The kinetic break as indicated by the plots of Figure 2 is facilitated by the increasing

imbalance between the heat supply and heat demand of a chemical reaction at the reaction interface [Kyobe, 2001]. The regulation of heat supply to the solid reactant at the reaction interface is achieved by the rise of temperature according to a pre-set heating programme. However, the pre-set heating programme is blind to the variation of heat demand of a chemical reaction at the contracting reaction interface. It should be noted that the measured rate constant is a kinetic response of the kinetic system to the undersupply/oversupply of heat to the reaction interface.

The shape of α - T curves (Fig. 1) reveals the effect of the cooling of the reaction, which is enhanced by the increase of the sample mass and heating rate. This fact is also reported as self-cooling/heating in the reports of the ICTAC Kinetics Project [Maciejewski, 2000, Brown, 1997]. The report discloses that self-cooling/heating increases with increasing sample mass causing the actual temperature of the reaction environment to differ from programmed heating temperature. This invalidates the decomposition kinetics of solid reverting to variable experimentally determined kinetic parameters. The frequency factor $A_s = 7.1 \times 10^{15}$ s^{-1} predicted according to equation (7) is the limiting value of the apparent frequency factor A' obtained when the decomposition proceeds free of self-cooling/heating.

Table 1: The kinetic measurements for the decompositions of 6 - 100 mg CaCO3 decomposed at different heating rates.

T (K)	5.969 mg (2.5) Kmin⁻¹	29.875 mg (2.5 Kmin⁻¹)		7.991 mg (3.5 Kmin⁻¹)					
	α	$d\alpha/dt \times 10^5$ s⁻¹	a cm²	α	$d\alpha/dt \times 10^5$ s⁻¹	a cm²	α	$d\alpha/dt \times 10^5$ s⁻¹	a cm²
843.15	0.00639	1.48787	0.08152						
848.75									
853.15	0.01150	2.17202	0.08124						
863.15	0.01917	3.11100	0.08082	0.00641	1.11350	0.23851			
873.15	0.02556	4.46362	0.08047	0.09615	1.55052	0.23800	0.00962	2.68203	0.09880
883.15	0.03834	5.95149	0.07976	0.01282	2.07160	0.23749	0.01604	3.71357	0.09838
888.15									
893.15	0.05431	7.70988	0.07887	0.01923	2.88510	0.23646	0.02244	4.99270	0.09795
903.15	0.07692	9.46828	0.07761	0.02885	4.08733	0.23491	0.03526	7.01454	0.09709
913.15	0.10224	14.6082	0.07619	0.03846	5.19380	0.23336	0.05128	9.30234	0.09601
923.15	0.13419	17.7192	0.07437	0.05128	6.79190	0.23128	0.07051	11.93126	0.09471
933.15	0.17308	20.8302	0.07212	0.07372	8.92270	0.22762	0.09295	14.96463	0.09318
943.15	0.21725	25.1586	0.06953	0.09615	10.7870	0.22393	0.12179	19.07105	0.09119
953.15	0.27796	29.2164	0.06589	0.12821	13.5840	0.21860	0.16026	23.66028	0.08851
963.15	0.33865	33.5448	0.06214	0.16026	16.7800	0.21321	0.20513	29.41216	0.08533
973.15	0.41534	37.6026	0.05724	0.21154	20.2430	0.20444	0.25641	35.88810	0.08162
978.15									
983.15	0.49840	40.4431	0.05168	0.25641	27.5900	0.19661	0.32051	41.69552	0.07686
988.15									
993.15	0.59425	41.5252	0.04487	0.32051	29.8240	0.18514	0.39103	48.39254	0.07144
998.15	0.64462	41.7355	0.04107						
1003.15	0.69010	41.7694	0.03749	0.38462	31.8290	0.17330	0.47436	52.68798	0.06477
1008.15	0.74380	40.7024	0.03302						
1013.15	0.78594	39.0905	0.02929	0.46795	35.8240	0.15728	0.58333	59.53894	0.05548
1018.15	0.83058	37.3967	0.02507						
1023.15	0.88174	31.5827	0.01972	0.55055	39.9886	0.13771	0.68910	62.36452	0.04564
1033.15				0.63842	40.88499	0.11368	0.79487	60.54808	0.03459
1037.15				0.69231	41.2842	0.10917			
1043.15				0.74359	40.3520	0.09668	0.89103	52.55573	0.02269
1053.15				0.852564	37.82166	0.06685	0.96795	33.70510	0.01003
1063.15				0.935897	31.1629	0.03837			

T (K)	7.997 mg (4.5)Kmin⁻¹	8.011 mg (4.0 Kmin⁻)		9.522 mg (2.0 Kmin⁻¹)					
	α	$d\alpha/dt \times 10^5$ (s⁻¹)	a (cm²)	α	$d\alpha/dt \times 10^5$ (s⁻¹)	a (cm²)	α	$d\alpha/dt \times 10^5$ (s⁻¹)	a (cm²)
833.15									
843.15							0.00637	1.23906	0.11129
853.15	0.00637	1.5388	0.09907				0.01274	1.80478	0.11082
863.15	0.00955	2.1085	0.09886				0.01592	2.50418	0.11058
873.15	0.01274	3.0478	0.09865	0.00635	2.49014	0.1301	0.02548	3.48230	0.10986
883.15	0.01911	4.2266	0.09822	0.01032	3.44718	0.1298	0.03822	4.48197	0.10890
893.15	0.02548	5.7849	0.09780	0.01542	4.65000	0.1293	0.05414	6.26810	0.10770
903.15	0.03822	7.8585	0.09694	0.02135	6.24700	0.1288	0.07643	7.98053	0.10600
913.15	0.05096	10.4810	0.09608	0.03492	8.53652	0.1276	0.10191	10.76502	0.10404
923.15	0.06688	13.9590	0.09500	0.05079	11.31414	0.1262	0.14013	13.43276	0.10107
933.15	0.08972	18.3450	0.09345	0.06984	14.08103	0.1245	0.17834	16.20884	0.098051
938.15							0.19745	17.63530	0.096525
943.15	0.10828	23.5650	0.09217	0.08889	17.49450	0.1228	0.23567	19.95580	0.093435
948.15							0.27796	21.34800	0.089956
953.15	0.14968	28.5790	0.08930	0.12381	23.10734	0.1197	0.29936	23.66850	0.088170
963.15	0.19108	35.0970	0.08638	0.16508	28.54438	0.1159	0.36943	27.16210	0.082189
973.15	0.24204	42.1170	0.08271	0.20952	33.52831	0.1117	0.46178	29.88913	0.073954
978.15	0.26752	45.6266	0.08084						
983.15	0.29299	48.1527	0.07896	0.26667	40.32458	0.1063	0.56394	32.57653	0.064272
988.15	0.33121	52.0952	0.07609						
993.15	0.34076	55.9563	0.07536	0.33016	47.57396	0.1001	0.66879	35.86801	0.053505
1003.15	0.42042	64.6767	0.06916	0.40000	53.29377	0.0930	0.77070	35.05540	0.041872
1013.15	0.50616	71.6962	0.06216	0.49524	55.17853	0.0828	0.85987	31.22480	0.030154
1023.15	0.62041	75.1405	0.05216	0.59048	57.94556	0.0721	0.94586	23.67980	0.015996
1030.15									
1031.15	0.70204	77.9663	0.04438						
1033.15	0.72653	75.4709	0.04192	0.69841	59.78777	0.0588			
1035.15				0.71111	60.70289	0.0571			
1043.15	0.84713	72.7017	0.02844	0.79365	56.24094	0.0456			
1053.15	0.93312	59.1642	0.01639	0.88888	47.58152	0.0302			
1063.15				0.96508	40.32458	0.0140			

Following the failure of the applied heating programme to adjust to the heat demand of the chemical reaction, the measured rate constant k_m would increase rapidly as a result of the excess heat supply Δq at the reaction interface. It should be noted that the influence of Δq makes the rate constant k_m to be larger than the Arrhenius rate constant k_T. The Arrhenius kinetic regime prevails only for $k_m/k_T < 1$, while it fails to be applicable in the acceleratory kinetic regime, when $k_m/k_T > 1$. This suggests that the correction for the effect of excess heat supply on the measured rate constant is of paramount importance (Kyobe, 2001). The relationship between the rate constant k_m in the acceleratory kinetic regime and Arrhenius rate constant k_T is described by the empirical equation (9) shown below;

$$k_m = k_T f(\Delta q) \qquad (9)$$

In equation (9), $f(\Delta q)$ is a function of the excess heat supply to the reaction interface. The excess heat Δq increases the fractional heat supply from 1 to $1 + \Delta q/q_o = (2 - aT/a_oT_o)$, which suggests

that the rate constant k_m must be dependent on this function. Based on experimental data, equation (9) is modified to equation (10),

$$k_m = k_T C_o \exp\left\{ y\left(2 - \frac{aT}{a_o T_o}\right)^2 \right\} \qquad (10)$$

where C_o and y are thermal transport parameters, which are found to vary from one sample to another. The plots of $\ln(k_m/k_T)$ vs $(2 - aT/a_oT_o)^2$ are shown in Figure 3 covering the entire acceleratory kinetic regime. The rate constants k_T determined according to equation (10) are used to extend the Arrhenius plots giving the same apparent kinetic parameters as those obtained earlier according to Figure 2. If in the rate equation (3) $E_a' = E_a - a_oRT_o$ is substituted followed by rearrangement, equation (11) is obtained,

$$k' = \frac{d\alpha}{dt}\frac{a_o}{a}\left\{ \frac{\exp\left(-a_o T_o\big/T\right)}{f(\alpha)} \right\} = A'\exp\left(\frac{-E_a}{RT}\right) \qquad (11)$$

Equation (11) allows the activation energy E_a for the chemical reaction to be determined directly from the kinetic measurements. Results according to this equation (11) are presented in Table 2.
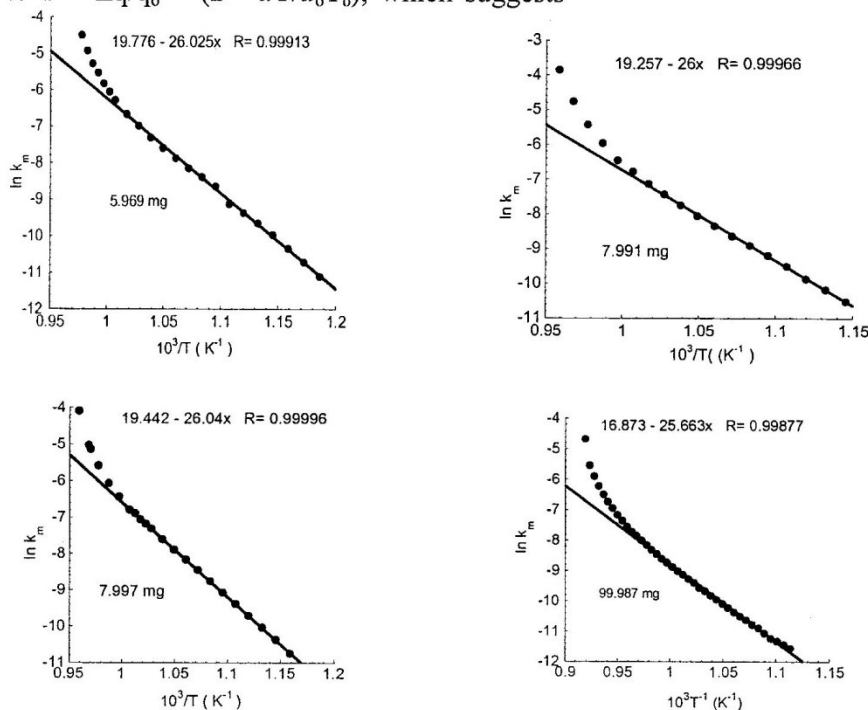

Figure 2. Plots of $l_n k_m$ vs 1/T for selected decompositions of $CaCO_3$ indicating the linear nature of the initial stage of decomposition followed by a subsequent rapid chemical reaction.

It is important however, to note that the effect of the cooling of the reaction environment is quite significant, particularly at high heating rates. The cooling of the reaction environment promotes the reverse

Table 2: Experimentally determined values of E_a/R ($E_a = 217$ kJmol^{-1}) directly from the kinetic measurements for the decomposition of $CaCO_3$ according to equation (11).

Sample mass (mg)	Heating Rate (Kmin^{-1})	E_a/R (K)
5.969	2.5	26091
6.016	1.5	26087
7.991	3.5	26079
7.997	4.5	26119
8.011	4.0	26103
8.015	2.5	26109
9.522	2.0	26092
12.039	4.0	26089
24.698	2.0	26099
29.875	2.5	26101
75.161	2.0	26092
99.987	2.0	26091

reaction thereby reducing both the values of A' and E_a'. Apparently the opposite effect is promoted by high heating rates (self-heating). When a small sample is decomposed at high heating rate, the reaction become dominated by self-heating. To demonstrate this point the experimental kinetic measurements according to Gallagher and Johnson [1973] and Elder and Reddy [1986] are revised. Elder and Reddy, decomposed a 3.7 mg $CaCO_3$ powder at the

heating rate from 10 to 50 K/min^{-1} in a stream of a nitrogen. The kinetic measurements for the heating rate of 10 K/min are shown in Table 3.

The solutions of the natural logarithmic form of equation (10) are the thermal transport parameters $\ln C_o = 3.7134$ and $y = 1.1564$ (Figure 4). Based on those solutions, the values of rate constant k_T corrected for the effect of self-heating are included in Table 3.

When the rate equation (3) is applied to the kinetic data in Table 3 assuming a first order reaction, $E_a' = 254$ kJ/mol is obtained from the linear part of the Arrhenius plot (Figure 5a). On the other hand, Gallagher and Johnson(1973) decomposed a 4 mg sample at the heating rate of5 K/min under flowing nitrogen and obtained $E_a' = 217.5$ kJ/mol. Since the sample mass of 3.7 mg and 4 are nearly equal, the difference between the results can be associated with self-heating, which is amplified by the high heating rate. The self-heating always tend to make the measured rate constant k_m (Table 3) larger than the Arrhenius rate constant k_T.
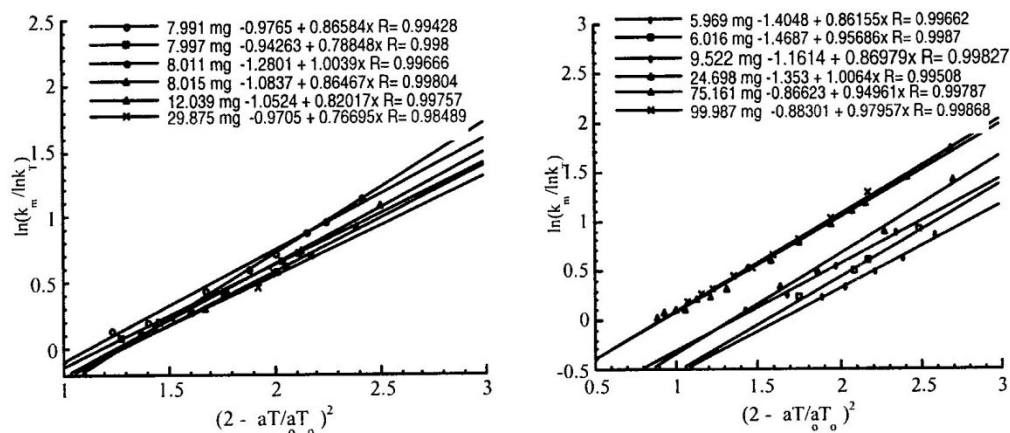

Figure. 3. Plots of $l_n(k_m/kT)$ against $(2 - aT/a_oT_o)^2$ for all samples accounting for the effect of excess heat supply to the subsequent chemical reaction as observed in Figure 2.

Table 3: The kinetic measurements for a 3.70 mg sample of $CaCO_3$ decomposed at the heating rate of 10 $Kmin^{-1}$ according to Elder and Reddy (1986).

T (K)	1 - α	$(d\alpha/dt) \times 10^3$ (min^{-1})	a (cm^2)	$k_m \times 10^3$ (min^{-1})	$k_T \times 10^5$ (min^{-1})
863.15	0.9960	3.11	0.05934	3.1308	2.8604
883.15	0.9869	7.41 .	0.05899	7.5747	7.1921
893.15	0.9789	9.68	0.05860	10.0302	9.6518
908.15	0.9588	15.91	0.05787	17.0657	16.5281
918.15	0.9398	22.19	0.05710	24.6092	23.7040
928.15	0.9147	29.70	0.05608	34.4585	32.6471
948.15	0.8333	52.59	0.05270	71.2690	61.4727
958.15	0.7751	65.52	0.05022	100.1792	79.1880
968.15	0.7038	75.54	0.04709	135.6526	94.6552
983.15	0.5643	104.6	0.04064	271.4449	140.0944
988.15	0.5090	113.71	0.03794	350.4309	156.8847
993.15	0.4508	121.29	0.03499	457.6342	173.6488
998.15	0.3876	130.05	0.03160	631.1570	195.8904
1003.15	0.3213	135.61	0.02792	899.7196	219.924
1008.15	0.2520	140.77	0.02375	1400.1543	256.6321
1013.15	0.1817	135.67	0.01909	2378.9810	308.6756

$$3.7134 + 1.1564x \quad R = 0.9979$$
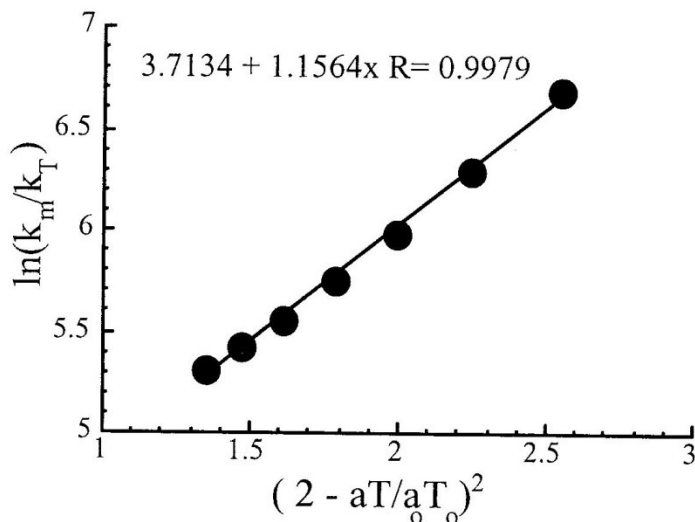
Figure 4: The dependence of $l_n(k_m/kT)$ on $(2 - aT/a_oT_o)^2$ for the decomposition of 3.7 mg $CaCO_3$ sample.

In assessing the significance of the thermal transport parameters the corrected data in Table 3 is used and the resulting plot (Figure 5b) gives $\ln A' = 19.897$ as intercept and $E_a'/R = 26016$ K as slope. The apparent activation energy $E_a' = 216.3$ kJ/mol is derived, which compares favourably with 217.5 kJ/mol as reported by Gallagher and Johnson (1973).

The Heat Imbalance

The arguments in the previous paragraphs can be summarised to mean that there is an imbalance between the heat supply and heat demand for the chemical reaction at the reaction interface. This distorts the decomposition kinetics of the solids leading to variable kinetic parameters. In Figure 6(a) is shown the plot of $\ln A'$ vs a_o according to equation (4) using the result of Figure 2. The closed circles show samples that were decomposed at low heating rates while the open circles represent samples, which were decomposed at higher heating rates. For samples heated at relatively high heating rates, the values of ln A' are depressed from the line of the best fit, which gives $\ln A = 20.277$ and $x = -6.5254$ cm^{-2}. The deviations of $\ln A'$ indicate that when heat is extracted from the reaction environment at a higher rate than the rate of heat flow to the reaction interface, the increase of heating rate will tend to reinforce the effect of the cooling of the reaction environment resulting into the drop of $\ln A'$. This view is again supported by the α - T plot of Figure 1, which shows the increase of heating rate to shift the

decomposition to higher temperature similar to the effect of sample mass. Shown in Figure 6(b) is the plot of E_a' vs a_o according to equation (5). The slope $RT_o = 6636.8$ J represent the heat, which is extracted from the reaction environment per cm^2 of the reaction interface. This slope give $T_o = 798.24$ K as the temperature at which the first decomposition was detected. The intercept $E_a = 216950$ $Jmol^{-1}$ is the activation energy derived.

The decrease $\Delta \ln A'$ of the apparent frequency factor A' by the increase of heating rate is accompanied by a corresponding decrease of the rate constant by an amount $\Delta \ln k$. In Table 4 are shown the differences $\Delta \ln k$ of the rate constant calculated on the basis of experimentally determined kinetic parameters (Figure 2) and those calculated using the results of Figure 6 at the temperature T_o.

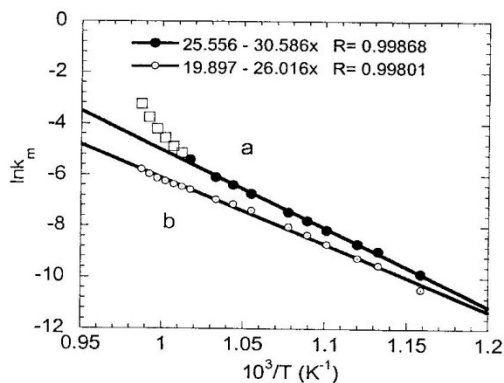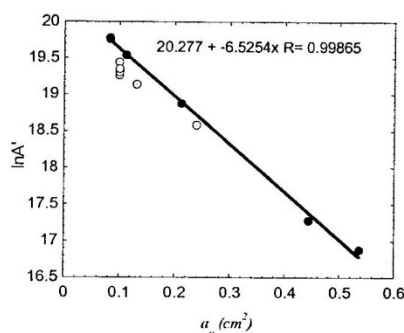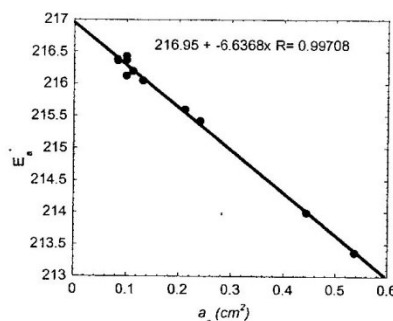Results presented in Table 4 show large values

(a)

(b)

Figure 6. Plots of (a) $\ln A'$ vs a_o and (b) E_a' vs a_o for the decomposition of a selected sample. The open circles, which show appreciable deviations from the line of the best fit, are data points for the sample masses that were decomposed at high heating rates.

Figure 5: The Arrhenius plot for the decomposition of a 3.7 mg $CaCO_3$ at the heating rate of 10 °C/min according to the kinetic measurements of Elder et al. The results in (a) shows the usual kinetic splitting and the distortion of the decomposition kinetics by high heating rate leading to high activation energy and in (b) the correction of the distortion by means of equation (10) eliminates the kinetic splitting.

of $\Delta \ln k$ for samples, which were decomposed at relatively high heating rates. The data points show significant deviation from the line of the best fit (Figure 6a). When a revised plot of $\ln A'$ vs a_o is constructed, the best line including all data point is obtained. The plot is shown in

Figure 7 with improved correlation coefficient from R = 0.99868 to 0.99991 giving $\ln A$ =20.283 and x = -6.5429 cm^{-2} as intercept and slope, respectively.

The linear dependencies of $\ln A'$ and E_a' on the area a_o of the reaction interface as suggested by equations (4) and (5) are limited to certain conditions. The equations are reasonably accurate for small sample mass and low heating rate. The value of $\ln A$ free from the effect of heat imbalance and sample randomness is obtained when equation (4) is modified to equation (12)

$$\ln A' = \ln A + a_o X + \Delta_c \qquad (12)$$

where Δ_c is a correction factor for the effect of heat imbalance, which decreases with decreasing sample mass and heating rates. In principle, during the progress of the chemical reaction of a solid reactant, an increasing layer of a solid reaction product forms around a contracting reaction interface. With the rise of temperature, the layer consumes an increasing fraction of the heat supply proportionate to its internal energy, while the heat demand at the reaction interface decreases. This suggests that the incident heat at the reaction interface is bound to decrease steadily up to a minimum before rising when the heat demand starts to decrease rapidly than the pace at which heat is consumed by the solid reaction product. Figure 8 is a sketch showing how the heat supply q_s and heat demand q_T varies with temperature. According to Figure 8, it is noted that the mechanism function $f(\alpha)$ satisfying the decomposition severity from the beginning up to the end cannot hold satisfactorily. The imbalance between the heat supply and heat demand at the reaction interface would, therefore, lead to an error in the estimation of $\ln A$ at $a_o = 0$.
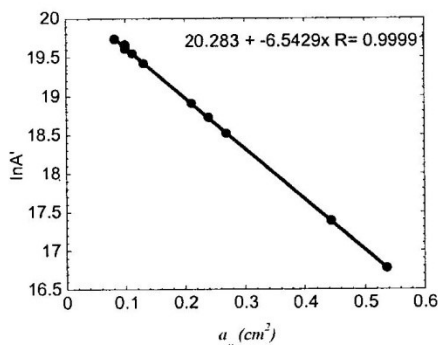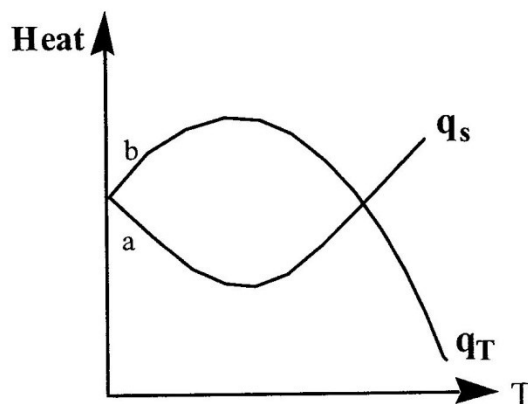

Figure 8. The variation of heat supply q_s and heat demand q_T with temperature.
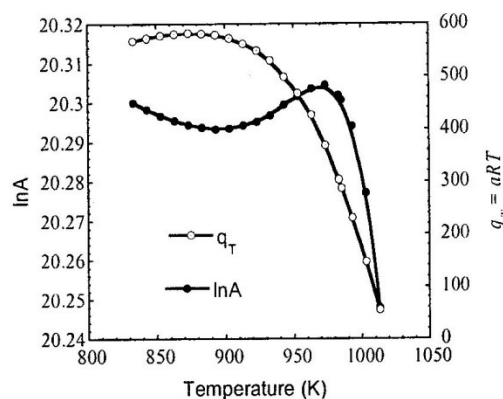

Figure 9: The variations of the heat demand q_T and $\ln A$ with temperature. The plots show minimum of $\ln A$ to be displaced by an amount $\Delta \ln A$ relative to the maximum of heat demand. The maximum of heat demand and maximum of heat supply fails to coincide following the effect of the cooling of the reaction environment.

Figure 7: A revised plot of $\ln A'$ against a_o when the effect of heating rate on A' was corrected.

In equation (12), the correction factor Δ_c is meaningful only when the same value of $\ln A$ for all temperatures is obtained. Accordingly when there is a balance between heat supply and heat demand at the reaction interface, all samples would give maximum heat demand at the same temperature T_M irrespective of the sample mass. However, this is not the case since the maximum heat demand is found to shift to higher

Table 4: The effect of heating rate on the frequency factor manifested by the decrease of the rate constant $\Delta \ln k$ at the threshold temperature T_o.

Sample mass (mg)	a_o (cm²)	$\ln A'$	E_a'/R (K)	Values of lnk at T_o		$\Delta \ln k$
				Calculated	Experimental	
5.969	0.0818664	19.776	26025	-12.86426	-12.82698	-0.03728
6.016	0.0822955	19.756	26022	-12.86663	-12.82698	-0.02341
7.991	0.099443	19.257	26000	-12.96137	-13.31466	0.35328
7.997	0.0994928	19.443	26040	-12.96165	-13.17877	0.21712
8.011	0.0996084	19.305	26024	-12.96229	-13.29672	0.33443
8.015	09964151	19.349	26029	-12.96247	-13.25899	0.29651
9.522	0.1117695	19.536	26003	-13.02948	-13.03942	0.00993
12.039	0.1306868	19.136	25989	-13.13401	-13.42188	0.28787
24.698	0.2106000	18.876	25931	-13.5776	-13.60922	0.03146
29.875	0.2395392	18.582	25910	-13.73546	-13.87691	0.14145
75.161	0.4430979	17.277	25738	-14.86021	-14.96644	0.10623
99.987	0.5359151	16.873	25663	-15.37311	-15.27648	0.09684

temperature T_M. Generally, the maximum heat demand is supposed to coincide with the minimum heat supply at which lnA is a minimum. But surprisingly it is observed that the minimum value of lnA is displaced by an amount $\Delta \ln A$ relative to the maximum heat demand. The displacement can be estimated from equation (13),

$$\Delta \ln A = \alpha_m \left(2 - \frac{a_m T_m}{a_o T_o} \right) - \alpha_M \left(2 - \frac{a_M T_M}{a_o T_o} \right) \ldots (13)$$

which is referred to as the correction factor Δ_c in equation (12). In equation (13), a_m and a_M are areas of the reaction interface at the temperatures T_m and T_M, respectively. The maximum heat demand is at the temperature T_M while minimum of lnA is at the temperature $T_m > T_M$. For any temperature T, at which a is the area of the reaction interface, the displacement $\Delta \ln A$ of lnA is an error emanating from the heat imbalance. Hence equation (12) modifies to:

$$\ln A = \ln A' + a_o x + \alpha_m \left(2 - \frac{a_m T_m}{a_o T_o} \right) - \alpha_M \left(2 - \frac{a_M T_M}{a_o T_o} \right) \ldots (14)$$

It should be noted that the minimum of lnA is always at a higher temperature $T_m > T_M$ in

Table 6: The Arrhenius kinetic parameters for the decomposition kinetics of various sample masses of calcite decomposed at different heating rates.

Sample mass (mg)	Arrhenius Kinetic Parameters	
	lnA	E_a/R (K)
5.969	20.333	26099
6.016	20.324	26111
7.991	20.33	26144
7.997	20.344	26145
8.015	20.333	26138
8.011	20.334	26141
9.522	20.330	26139
12.039	20.340	26142
24.698	20.384	26199
29.875	20.401	26193
75.161	20.352	26237
99.987	20.631	26299

consistency with the effect of the cooling of the reaction environment on the decomposition temperature. To identify the temperature T_m at which lnA is a minimum, the plots of q_T and lnA vs T are constructed. The representative plots are shown in Figure 9.

In equation (14) the values of lnA' of Figure 2 and x = 6.5429 (slope of Figure 7) are used. The results are summarized in Table 5. By making use of E_a/R values listed in Table 2 and lnA from Table 5, the plots of $lnk_o = lnA - E_a/RT$ vs $1/T$ are constructed and results are summarized in Table 6. The results in Table 6 give lnA = 20.369 and E_a/R = 26162.25 K as average values from which the frequency factor, A = 7.0 x 10^8 s^{-1} and the activation energy, E_a = 217.5 kJmol^{-1} are obtained for the decomposition of $CaCO_3$ according to a first order chemical reaction

CONCLUSION

It has been established that the traditional rate equation (1) frequently applied to kinetic studies of solid state decompositions does not satisfy the requirements for interface chemical reaction. This is because in the rate equation the kinetic system is not defined. Since the kinetic system in the present study is defined on the basis of kinetic measurement referred to as the population N_s localised at the reaction interface, the rate equation (1) is abandoned in favour of

comparison makes it possible to show that the decomposition of $CaCO_3$ is a first order reaction and the kinetic parameters A = 7.0 x 10^8 s^{-1} and E_a = 217.5 kJmol^{-1} are thereby concluded.

Prior to this study, a number of investigators have paid greater emphasis only to controlling the pressure and the effect of gaseous reaction products. The effect of the cooling of the reaction environment, which makes heat transport a preferred rate limiting process, was always underrated. For this reason the results have always deviated from the real kinetic parameters A and E_a of a chemical rate-determining step. The effects of heat transport impose restrictions to the sample mass and heating rates that can be employed in meaningful experimental kinetic studies of solid state decompositions. The failures to observe and contain those restrictions invariably lead to incorrect inference of the reaction mechanism and the kinetic parameters.

ACKNOWLEDGEMENT

Table 5: The summary of the variation of values of lnA with E_a upon consideration of the heat index.

Heating Rate (K/min)	Sample mass (mg)	lnA	E_a/R (K)
2.5	5.969	20.323	26099
1.5	6.016	20.324	26111
3.5	7.991	20.333	26144
4.5	7.997	20.344	26145
2.5	8.015	20.333	26138
4.0	8.110	20.334	26141
2.0	9.522	20.330	26139
4.0	12.039	20.340	26142
2.0	24.698	20.383	25199
2.5	29.875	20.401	26193
2.0	75.161	20.362	26237
2.0	99.987	20.631	26299

equation (3). By so doing the comparison of solid state decompositions and those of gas phase chemical reactions can be done. The

REFERENCES

1. Berlin, A. and Robinson, R. J., *Anal. Chem. Acta.* **27** (1962) 68.

2. Beruto, D. and Searcy, A. W., *J. Chem. Soc. Faraday Trans.*, I, **70** (1974) 2145.

3. Britton, H. T. S, Gregg, S. J. and Windson, G. W., *Trans. Farad Soc.*, **48** (1952) 63.

4. Brown, M. E., *J. Therm. Anal.* **49** (1997) 17.

5. Daniels, F., *Ann. Rev. Phys. Chem.*, **1** (1980) 233.

6. Dollimore, D., Reading, M., Rouquerol, J., and Rouquerol, F., *J Therm. Anal.* **29** (1984) 775.

7. Dowdy, D. R., *J. Therm. Anal.*, **32** (1987) 137.

8. Doyle, C. D., *J. Appl. Polymer Sci.*, **6** (1962) 639.

9. Drapper, A. L. and Sveum, L. K., *Thermochim. Acta.* **1**, (1970) 345.

10. Elder, J. P. and Reddy, V. B., *J. Therm. Anal.*, 31 (1986) 395.

11. Gallagher, P. K. and Johnson, D. W. Jr., *Thermochim. Acta.*, **6** (1973) 67.

12. Garn, P. D., *J. Therm. Anal.*, **13** (1978) 581.

13. Guler, G., Dollimore, D. and Heal, C. R., *Thermochim. Acta*, **54** (1982) 187.

14. Ingraham, T. R. and Marier, P., *Canad. J Chem. Eng.*, **41** (1963) 170.

15. Kyobe, J. P. W., M.Sc. Thesis, University of Dar es Salaam, (2001).

16. Lide, D. R, (Ed in Chief), *C. R. C Handbook of Chemistry and Physics*, 73rd Ed., CRC Press, Ann Arbor, (1992).

17. Maciejewski, M., *Computational Aspects of Kinetic Analysis*, Part B of ICTAC Kinetics Project, CH8092, Zurich (2000).

18. Rouquerol, F. and Rouquerol, J., in *Proc. of 3rd ICTA Conf.* Edited by Wiedmann, H. G., Vol. 1, p. 373, Birkhäuser, Stuttgart (1972).

19. Speros, D. M. and Woodhouse, R. L,. *J. Phys Chem.*, **72** (1968) 2846.

20. Szwarc, M., *J. Phys & Colloidal Chem.*, **1** (1961) 53.

21. Trotman-Dickenson. A. F *Ann. Rev. Chem.*, **10** (1959) 53.

22. Waters. W. D., *Ann. Rev. Phys. Chem.*, **12** (1961) 411.

23. Wells, A. F., *Structural Inorganic Chemistry*, 3rd Ed., Oxford Press, Oxford, 1962

NOTES FOR AUTHORS

UHANDISI PUBLICATIONS of the College of Engineering and Technology, University of Dar es Salaam is published to disseminate results and findings of research work conducted by engineers and scientists.

The journal includes refereed papers of original work, state-of-the-art reviews, articles of emerging areas that could stimulate new research, technical notes and letters to the editor. The criterion for inclusion of any item the journal is that it should be useful or interesting to the scientific community.

The editorial policy of Uhandisi Publications is not only to find and publish appropriate materials, but also to ensure that the information is presented in a practical and convenient manner.

1. Manuscript submission

Three copies of the manuscript (prepared according to the instructions below) should be sent to the Chief Editor, Uhandisi Publications, P. O. Box 35131, Dar es Salaam, Telephone: (*) 255 22 2410368; Fax: (*) 255 22 2410379; E-mail: atemu@cpe.udsm.ac.tz. The manuscript must be in its final form. Please retain original figures until the review process has been completed. Include with the revised manuscript reproducible copies of any figures and a disk with an MS-WORD copy of the paper. All accepted manuscripts become the property of the publisher.

2. Manuscript preparation

All manuscripts must be typed double-spaced on only one side of the paper with margins of 3 cm all round. The following points should be adhered to in the preparation of the manuscript:

Title, Authors, and Affiliation: The manuscript should have a cover page containing a clear and concise title; the name and institutional affiliations of author(s); and the complete mailing address, telephone and fax numbers, and e-mail address of the person to whom all correspondences and proofs should be sent. The next page of the paper should start with the title followed by the Abstract.

Abstract: Every paper must have an abstract of no more than 150 words. This is not necessary for technical notes.

Keywords: Important keywords, to be used for online search and retrieval, as well as indexing must be included just after the abstract.

Introduction. The Introduction should explain the purpose of the study, cite relevant work and describe the objectives.

Body. The body presents the details of the study. It may be broken down into several sections, which should be identified with descriptive headings that are not numbered. Appropriate figures and tables may be used to support the discussion. Examples of headings are: Theory, Experimental work, and Results and Discussion.

Conclusions and Recommendations: Point out the significance of the work, its limitations and advantages, application of the results and recommendations.

Acknowledgement. Acknowledge any support to the work.

Nomenclature. Should list all the symbols used in alphabetical order, giving definitions, and units in metric system. Greek letters, subscripts, and superscripts should be included.

References. Should be cited in the manuscript by using *Name and Year* system. Reference listing at the end of the manuscript should be in alphabetical order and in the following format

Journal articles: Kisamo, J. D., and E.A. Kitumbi, *Thin Layer Drying of Diced Cassava Roots*, Uhandisi Journal, Vol. 22 No. 1, pp 13-25,1998.

Book: Fletcher, C. J. *Computational Techniques for Fluid Dynamics*, 3rd Ed., Vol. I, pp.120 – 220, Springer-Verlag, New York, 1991.

Conference proceedings: Kandlikar, S. G. *Boling Heat Transfer with Binary Mixtures*, Proc. 32nd National Heat Transfer Conf., Baltmore, Vol. 342, pp. 19-26, 1997

Refrain from using URL references. If a reference has been obtained from the Internet the address should be given: E.g. [http://www.udsm.ac.tz/article.html].

3. Figures

All figures should carry consecutive Arabic numbers, with descriptive captions, and be referred to in the text. Keep figures separate from the text, but indicate an approximate position for each in the margin.

Preparation: Figures submitted must be of high quality for direct reproduction. Line drawings should be prepared in black (India) ink on white paper or on tracing paper, with legend included. Alternatively, good sharp photo-prints are acceptable. Photographs intended for halftone reproduction must be good glossy original prints, of maximum contrast. Clearly label each figure with author's name and figure number; indicate "top" where this is not obvious.

Size: The preferred width of submitted line drawings is 18 to 20 cm with capital lettering 4 mm high, to accommodate reduction to single-column width.

4. Equations and Formulae

Mathematical: All symbols in equations must be clear. Identify unconventional or ambiguous symbols in the margin when they first appear. Underline vectors with a wavy line.

Chemical: Supply reproducible artwork for chemical equations. Long reaction sequences should be treated like figures.

5. Tables

Number tables consecutively with roman numerals, and give each a clear descriptive caption at the top.

Table 1 Sample table, typical values of Beta coefficients

Beta	Value at 200 K	Value at 300 K	Value at 600 K
1	0.3	0.6	0.5
2	0.4	0.8	0.8

6. Footnotes

A footnote may include the designation of a corresponding author of the paper, current address information for an author (if different from that shown in the affiliation). Footnotes should be indicated in the text by the following symbols: (*,+,++,§,||,#). Type footnotes to a table directly beneath the table.

7. Offprints

Each author of an article will receive a complete copy of the issue in which the article appears, up to a total of 3 copies per article. The corresponding author is responsible for distribution of copies to coauthors.